

The Crystal Structure of $\text{Ag}_2\text{IF} \cdot \text{H}_2\text{O}$ —A Compound Containing Ag_2^{2+} Pairs

KENNETH PERSSON AND BERTIL HOLMBERG

Physical Chemistry 1, Chemical Center, University of Lund, P.O. Box 740, S-220 07 Lund 7, Sweden

Received September 10, 1981; in revised form November 9, 1981

$\text{Ag}_2\text{IF} \cdot \text{H}_2\text{O}$ is monoclinic, space group $P2_1$, with $a = 4.7206(5)$, $b = 7.8117(8)$, $c = 6.3747(4)$ Å, $\beta = 93.345(9)^\circ$, $Z = 2$, $D_m = 5.35$, and $D_x = 5.37$ Mg m $^{-3}$. The structure was determined from single-crystal X-ray and neutron diffractometer data. X-Ray data were refined anisotropically to an R value of 0.033. The Ag atoms are grouped together in Ag_2^{2+} pairs with very short (2.81 Å) Ag–Ag distances. X-Ray photoelectron spectra do not reveal, however, any significant effect on the Ag electron-binding energy due to a possible metallic Ag–Ag interaction. The I atom has four nearest Ag neighbors (two Ag_2 pairs) describing a distorted square pyramid with the I atom in the top. These square pyramids are linked up to chains via shared edges. Each Ag atom has a tetrahedral anionic surrounding of O, F, and I atoms. These tetrahedra share edges and corners, creating sheets which are linked by a system of comparably short hydrogen bonds between the O and F atoms.

Introduction

A number of materials of composition $\text{Ag}_n\text{X}_x\text{A}_y$ ($n > x$), with $X = \text{Cl}$, Br , or I and various oxoanions A , can be obtained as crystalline compounds, whereas others have been characterized as high-conductivity glasses (1). For compounds belonging to the first class, the crystal structure is now known for Ag_2XNO_3 ($X = \text{Cl}$, Br , or I) (2–4), $\text{Ag}_3\text{I}(\text{NO}_3)_2$ (5), $\text{Ag}_3\text{I}(\text{ClO}_4)_2 \cdot 2\text{H}_2\text{O}$ (6), and $\text{Ag}_{26}\text{I}_{18}\text{W}_4\text{O}_{16}$ (7), an ionic conductor. A mixed $\text{Ag}(\text{I})$ – $\text{Hg}(\text{II})$ compound, $\text{Ag}_2\text{HgI}_2(\text{NO}_3)_2 \cdot \text{H}_2\text{O}$, has also been structurally characterized (8). The fact that cationic halide complexes $\text{Ag}_n\text{X}^{(n-1)+}$ have been detected in concentrated aqueous electrolyte solutions and molten salt systems (9) suggests that the configuration of Ag around the halide X in these compounds might be largely determined by geometrical

demands of coordinate bonds of such complex units. It is clear now, as the structural evidence has emerged, that the coordination of Ag around X may change not only with the nature of X but also with the counterion A .

In order to further explore the role of the anion A in the structure of compounds $\text{Ag}_n\text{X}_x\text{A}_y$ with $n > x$, an attempt was made at this laboratory to synthesize single crystals of Ag_2IF . This compound has been reported by Lieser, and cell dimensions as well as suggestions of probable space groups have been given (10). In addition a dihydrate, $\text{Ag}_2\text{IF} \cdot 2\text{H}_2\text{O}$, has been reported earlier (11).

A closer investigation of the solids formed in the system AgI – AgF – H_2O showed, however, that the compound described by Lieser is $\text{Ag}_2\text{IF} \cdot \text{H}_2\text{O}$. A very brief report on the structure has been given

(12). Another compound in this system, viz., $\text{Ag}_7\text{I}_2\text{F}_5 \cdot 2.5\text{H}_2\text{O}$, could also be synthesized and the structure has been solved (13). The existence of $\text{Ag}_2\text{IF} \cdot 2\text{H}_2\text{O}$ could not be confirmed, and it therefore seems probable that both "Ag₂IF" and "Ag₂IF · 2H₂O" are actually Ag₂IF · H₂O, the detailed structure of which will be described in this paper.

Experimental

A concentrated AgF solution was prepared by dissolution of Ag₂O in concn HF. This AgF solution was saturated with AgI at about 323 K, and after filtration single crystals of Ag₂IF · H₂O crystallized on cooling. The crystals were colorless to soft yellow and had the shape of oval plates.

The total silver content was determined by electroanalytical precipitation of Ag. Water analysis, based on coulometrically generated Karl Fischer reagent (14), is consistent with the composition Ag₂IF · H₂O ($\text{H}_2\text{O}_{\text{calcd}} = 4.74\%$; $\text{H}_2\text{O}_{\text{exp}} = 4.70\%$). The

density (D_m) was determined by the displacement method in benzene.

Ag₂IF · H₂O is very sensitive to moisture and decomposes in laboratory air to AgI and AgF. During the X-ray data collection the crystal was enclosed in a glass capillary. The surface of the crystal darkens when exposed to light but this had no serious effect on the X-ray intensities (see below).

X-Ray diffraction. Table I gives information concerning the crystal data, the collection of intensities, and the refinement. The method employed in the data collection has been described elsewhere (15). Weissenberg photos revealed the Laue class $2/m$ and the systematic absences $0k0: k = 2n + 1$, and thus two possible space groups, $P2_1$ or $P2_1/m$. A single-crystal diffractometer (CAD-4) was used for data collection and the cell dimensions were improved by least-squares refinement of 60 reflections (16). The wavelength used for the determination of the cell dimensions was 0.70930 Å.

The intensities of three reflections ($1\bar{1}3$,

TABLE I
CRYSTAL DATA, COLLECTION AND REDUCTION OF X-RAY INTENSITY DATA,
AND THE LEAST-SQUARES REFINEMENT

Ag ₂ IF · H ₂ O: F.W.	379.69	μ (MoK α) (mm ⁻¹)	14.64
Crystal system	Monoclinic	Range of transmission factor	0.243–0.642
Space group	$P2_1$	Number of measured reflections	820
a (Å)	4.7206(5)	Number of reflections given	76
b (Å)	7.8117(8)	zero weight	
c (Å)	6.3747(9)	Number of independent reflections	744
β (°)	93.345(9)	used in the final refinement, m	
Z	2	Number of parameters refined, n	46
D_x	5.37	$R = \Sigma F_o - F_c / \Sigma F_o $	0.033
D_m	5.35	$R_w = [\Sigma w(F_o - F_c)^2 / \Sigma F_o ^2]^{1/2}$	0.040
Crystal size (mm)	$0.113 \times 0.375 \times 0.030$	$S = [\Sigma w(F_o - F_c)^2 / (m - n)]^{1/2}$	1.24
Radiation (graphite monochromated)	MoK α ($\lambda = 0.71073$ Å)	a (weighting function)	0.016
Take-off angle (°)	3	b (weighting function)	0.4
$\Delta\omega$ (°) (ω - 2θ scan)	$0.70 + 0.50 \tan \theta$	$g \times 10^{-4}$ (extinction)	0.047(19)
$\Delta\theta$ (°)	3–30	Mosaic spread (sec of arc)	122
Minimum number of counts in a scan	3000	Domain size (mm)	0.34×10^{-4}
Maximum recording time (sec)	180		

$\bar{2}\bar{2}1$, $\bar{2}\bar{1}2$), checked after every 100th measurement, showed random fluctuation <4%. The values of I and $\sigma_c(I)$, where $\sigma_c(I)$ is the standard deviation based on counting statistics, were corrected for Lorentz, polarization, and absorption effects. The expression $p = (\cos^2 2\theta_M + \cos^2 2\theta)/(1 + \cos^2 2\theta_M)$, with $\theta_M = 6.08^\circ$, was used in the correction for polarization. The crystal shape was described by seven planes.

Neutron diffraction. Single-crystal neutron diffraction data from a crystal of about 10 mm^3 in volume were collected on a Hilger and Watts four-circle diffractometer at the Swedish Atomic Energy reactor R2, Studsvik. The neutron wavelength was 1.210 \AA , and the flux at the crystal was about $10^6 \text{ sec}^{-1} \text{ cm}^{-2}$. The intensities of 706 reflections with $\sin \theta/\lambda < 0.6930 \text{ \AA}^{-1}$ were recorded at room temperature. The ω - 2θ step scan technique was used. Three standard reflections (023, 221, 131) were measured at regular intervals (every 15th measurement). The variation of the intensities were <9% and showed a random fluctuation. The intensities were corrected for Lorentz and absorption effects. The value for the linear absorption coefficient was determined to be 1.17 cm^{-1} , corresponding to an incoherent scattering cross section for H of $26 b$. The transmission factor varied within the range of 0.745–0.867. The standard deviations, $\sigma_c(I)$, were estimated from counting statistics. The morphology of the crystal was described by eleven planes.

X-Ray photoelectron spectra. The XPS measurements were performed with an AEI ES 200 electron spectrometer with $\text{AlK}\alpha$ radiation. The samples were mounted on a Pt foil. The electron-binding energies given refer to $E_b(\text{C}1s) = 285.0 \text{ eV}$ from the pump oil contamination.

Structure Determination and Refinement

X-Ray Diffraction

The atomic positions for Ag and I were

determined by Patterson and Fourier techniques. The method of symbolic addition (17, 18) was used to obtain E statistics, which indicated the structure to be noncentrosymmetric. Hence the result was interpreted in space group $P2_1$. A difference synthesis revealed the positions of the O and F atoms. The hydrogen atoms could not be located and hence it was impossible to unambiguously distinguish between O and F in the structure.

Full-matrix least-squares refinement, minimizing $\sum w(|F_o| - |F_c|)^2$, was performed with weights $w = 1/[\sigma_c^2/(4F_o^2) + (aF_o)^2 + b]$. The applied constants a and b were chosen to make the average values $\langle w(|F_o| - |F_c|)^2 \rangle$ almost equal in different $|F_o|$ and $\sin \theta$ intervals. One scale factor, positional and anisotropic thermal parameters, were refined (Table I). Scattering factors were taken from International Tables for X-ray crystallography (19). The final refinement also included correction for extinction (20) and anomalous dispersion by

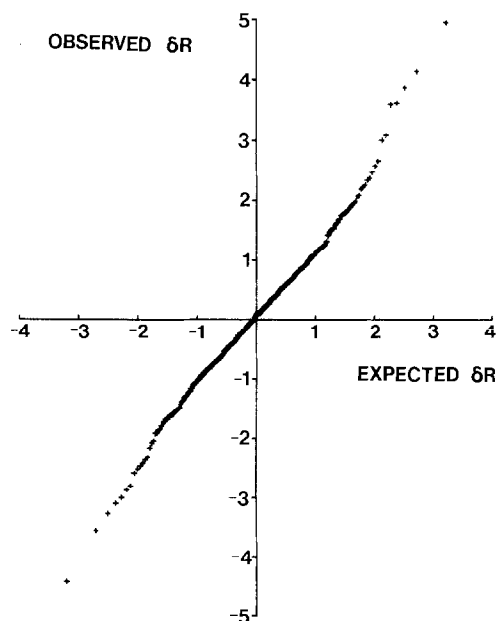


FIG. 1. Normal probability plot of 744 $\delta R(i)$ based on the structure factors.

TABLE II
POSITIONAL AND ISOTROPIC THERMAL PARAMETERS
WITH ESTIMATED STANDARD DEVIATIONS

Atom	x	y	z	B (Å ²)
	X-Ray			
Ag(1)	0.04256(33)	0	0.28550(23)	4.06(4)
Ag(2)	0.01611(32)	0.55975(21)	0.28428(22)	4.00(4)
I	0.32599(10)	0.28561(24)	0.49781(9)	2.31(1)
F	-0.2814(25)	0.4472(15)	0.0075(20)	3.3(3)
O	-0.2694(24)	0.1223(16)	0.0122(25)	2.8(3)
	Neutron			
Ag(1)	0.0416(33)	0	0.2886(17)	2.1(4)
Ag(2)	-0.0253(36)	0.5338(32)	0.2793(77)	8(1)
I	0.3333(23)	0.2758(28)	0.4912(25)	2.8(5)
F	-0.2801(32)	0.4501(27)	-0.0084(31)	2.1(5)
O	-0.2582(38)	0.1194(26)	0.0213(20)	3.1(6)
H(1)	0.6867(53)	0.2469(47)	0.0139(39)	4(1)
H(2)	0.536(15)	0.0367(87)	0.0107(81)	6(1)

Ag and I. No reflection had extinction correction $>4\%$ in $|F_0|$. In the last cycle the shift in the parameters was less than 1% of the estimated standard deviations and the refinement was considered complete. A final difference synthesis showed peaks of height $1.7 e \text{ \AA}^{-3}$ or less in the vicinity of the heavy atoms, but apart from this it was featureless. No probable positions of the H atoms appeared.

Figure 1 shows a normal probability plot of $\delta R(i) = ||F_0(i)| - |F_c(i)||/\sigma|F_0(i)|$ versus the values expected for a normal distribution (21). The slope and intercept of the least-squares line fitted to all data are 1.18 and 0.04, respectively. The value of the slope indicates that $\sigma(|F_0|)$ is underestimated by about 20%. It is still in good agreement, however, with the value of the ESD of an observation of unit weight ($S = 1.25$, Table I). Final positional and isotropic thermal parameters are given in Table II.¹

Neutron Diffraction

The positions of atoms, other than hydro-

¹ List of structure factors, anisotropic thermal parameters, and root-mean-square components of thermal displacement along the ellipsoid axes may be obtained by request to the authors.

gen, were taken from the X-ray study. A difference synthesis was performed after refinement of the scale factors ($R = 0.30$). It showed the positions of the two hydrogen atoms, which made it possible to discriminate between O and F. Full-matrix least-squares refinement was carried out as for the X-ray data. The coherent scattering amplitudes were taken from Bacon (22). Isotropic extinction correction was applied and the extinction coefficient g (20) was refined to a value of $6(2) \times 10^4$, which gave good agreement between the $|F_0|$ and $|F_c|$ for the reflections affected by extinction.

Reflections with intensities $\leq 3\sigma$ were given zero weight in the refinement. Of the remaining 280 reflections, 18 more were given zero weight because they seemed to be affected by multiple diffraction (23). These 18 reflections were checked for influence of multiple diffraction by calculating the possible reflections which could cause the observed increase in the F_0

TABLE III
SELECTED INTERATOMIC DISTANCES (Å) AND
ANGLES (°) FROM THE X-RAY DATA WITH
ESTIMATED STANDARD DEVIATIONS

Distances			
Ag(1)-I	2.832(2)		
Ag(1)-I	2.896(2)	I-I	4.237(1)
Ag(1)-I	3.622(2)	Ag(1)-Ag(2)	2.812(2)
Ag(1)-I	4.334(2)	Ag(1)-Ag(2)	3.441(2)
Ag(2)-I	2.813(2)	Ag(1)-Ag(2)	3.656(2)
Ag(2)-I	2.889(2)	O-H . . . F	2.52(2)
Ag(2)-I	3.766(2)	O-H . . . F	2.54(2)
Ag(2)-I	4.192(2)	O-F	2.95(2)
Ag(1)-F	2.27(1)	O-I	3.91(2)
Ag(2)-F	2.36(1)	O-I	3.94(1)
Ag(1)-O	2.41(1)	F-I	3.86(1)
Ag(2)-O	2.35(1)	F-I	3.93(1)
Angles			
I-Ag(1)-I	120.52(05)	I-Ag(2)-I	121.45(05)
I-Ag(1)-F	106.59(31)	I-Ag(2)-F	105.60(30)
I-Ag(1)-F	129.90(30)	I-Ag(2)-F	109.83(30)
I-Ag(1)-O	106.15(30)	I-Ag(2)-O	105.44(30)
I-Ag(1)-O	102.72(30)	I-Ag(2)-O	126.96(31)
F-Ag(1)-O	77.86(45)	F-Ag(2)-O	77.55(44)
O-F-O	116.45(50)	F-O-F	118.86(50)
O-F-O	119.19(63)	F-O-F	119.19(63)
O-F-O	124.14(55)	F-O-F	121.59(53)
Ag(2)-Ag(1)-Ag(2)	99.35(05)	Ag(2)-Ag(1)-Ag(2)	80.27(05)
Ag(1)-Ag(2)-Ag(1)	99.75(05)	Ag(1)-Ag(2)-Ag(1)	80.64(05)

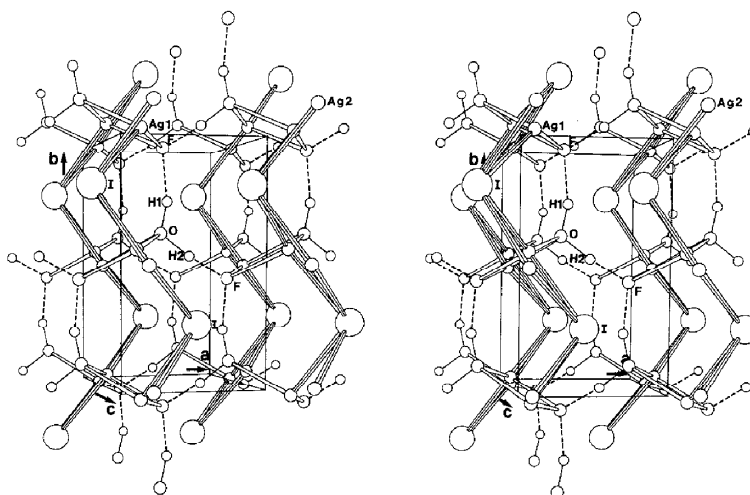


FIG. 2. A stereoscopic pair of drawings showing the contents of the unit cell based on the X-ray data. The H atom positions are taken from the neutron data. Figs. 2, 5, and 6 were drawn by the program ORTEP II (56).

values for weak intensities. In each case there was at least a combination of two strong reflections which might have caused the increase. The refinement thus based on 262 reflections converged to an R value of 0.09. As 65 parameters were refined, the ratio between the independent measurements (m) and parameters (n) was as small as 4.0. The relatively high R value, as compared to the X-ray investigation, might in part be attributed to some uncertainty in

the position of the Ag(2) atom, exhibiting a large thermal vibration ($B = 8(1) \text{ \AA}^2$, Table II). The low ratio m/n , 4.0, should also be considered (cf. $m/n = 16$ for the X-ray data). The constants a and b used in the weighting function were 0.05 and 0.02 and

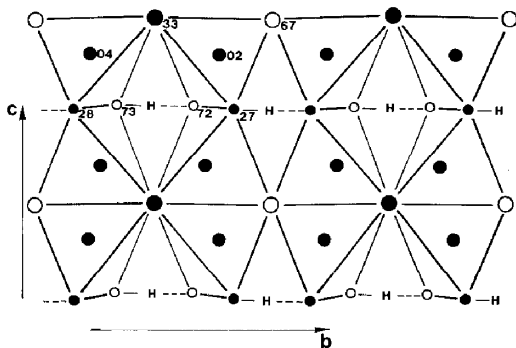


FIG. 3. A projection of the structure along a . Large circles are I, then Ag, and the smallest are F and O atoms. Open and solid circles denote the height along the projection axis.

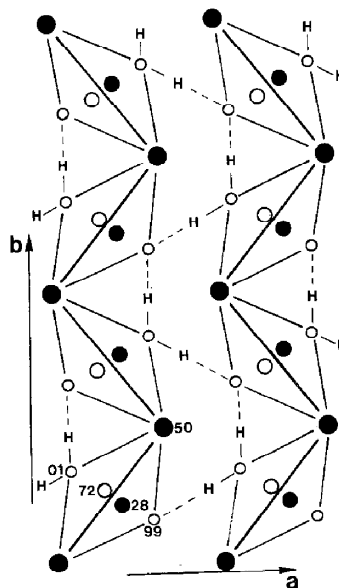


FIG. 4. A projection of the structure along c . The notations are according to Fig. 3.

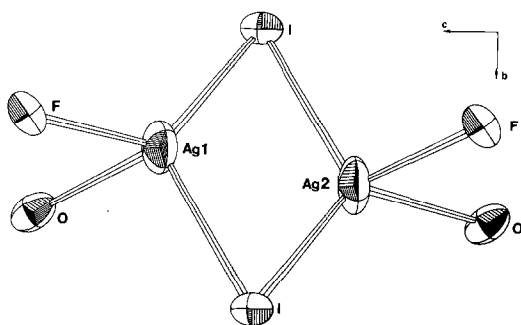


FIG. 5. The tetrahedra around Ag(1) and Ag(2), linked by an I-I edge. The thermal ellipsoids are scaled to include 50% probability in Figs. 5 and 6.

the S value equals 0.98. These quantities are defined in Table I. Two scale factors, positional and anisotropic thermal parameters, were refined. In the last cycle the shifts in the parameters for most atoms were $<2\%$ of the estimated standard deviations. The final positional and isotropic thermal parameters are given in Table II.¹

Description and Discussion of the Structure

General Feature

A stereoview of the unit cell is given in Fig. 2. Selected interatomic distances and angles are listed in Table III. The structure consists of layers in the bc plane held together by a hydrogen bond system . . . H-O-H . . . F in the ab plane, very close to $z = 0$. The layers are formed by distorted tetrahedra of one F, two I, and one O atom coordinated to Ag. The tetrahedra share edges along c and corners along b (Fig. 3).

Looking at the anions in $\text{Ag}_2\text{IF} \cdot \text{H}_2\text{O}$, the structure has great resemblance to the structure of Li_3N (24), which is the antitype of UO_3 (25). The O and F atoms build up a two-dimensional network of hexagons in the ab plane (Fig. 4). Between these hexagons I atoms are situated and empty hexagonal bipyramids, which share corners in the axial direction, are formed. All edges of the hexagon are shared with other hexagons.

Li_3N also contains those polyhedra with N atom as central atom and Li at all corners. The axis of the bipyramid is long ($= c = 6.37 \text{ \AA}$) and the Ag atoms are located between these layers of hexagons just outside 4 of the 12 triangular faces of the hexagonal bipyramid. They form, together with the I atoms, a chain along b .

Two tetrahedra containing Ag(1) and Ag(2) are joined via an I-I edge (Fig. 5). The tetrahedra are very distorted (Table III) as a consequence of the large difference in size of the atoms I, F, and O. The Ag(1)-Ag(2) distance within such a pair of tetrahedra is remarkably short, 2.81 \AA .

The Hydrogen Bond System

The layers of Ag containing tetrahedra are joined by a hydrogen bond system which involves distances O-H . . . F, which are noticeably short: 2.52 and 2.54 \AA from X-ray data. The corresponding distances from the neutron diffraction study are 2.51 and 2.59 \AA (Table IV), which, taking into consideration the standard deviations in the two structure refinements, is not significantly different from the X-ray results.

TABLE IV
SELECTED INTERATOMIC DISTANCES (\AA) AND ANGLES ($^\circ$) FROM THE NEUTRON INVESTIGATION WITH ESTIMATED STANDARD DEVIATIONS

		Distances
O-H . . . F		2.51(2)
O-H . . . F		2.59(3)
O-F		2.91(2)
O-H(1)		1.03(4)
O-H(2)		1.16(8)
F . . . H(1)		1.60(4)
F . . . H(2)		1.34(8)
H(1)-H(2)		1.79(8)
		Angles
H(1)-O-H(2)		109(4)
H(1) . . . F . . . H(2)		116(3)
O-H(1) . . . F		161(4)
O-H(2) . . . F		176(6)

These O–H . . . F distances are of the same order of magnitude as those found in $\text{Ag}_7\text{I}_2\text{F}_5 \cdot 2.5\text{H}_2\text{O}$ (13). Pimental and McClelland have given an average value of 2.72 Å for O–H . . . F bonds (26). The O–H . . . F distances in metal fluoride hydrates have an average value of 2.682 Å for a total of 46 hydrogen bonds and it is found that all known bonds of this type range from 2.56 to 2.86 Å (27). A theoretical calculation for $\text{H}_2\text{O}-\text{F}^-$ by Kistenmacher *et al.* (28), however, yielded the following dimensions: O . . . F = 2.52 Å and O–H . . . F = 173°. These results are consistent with the dimensions observed in the two structures $\text{Ag}_2\text{IF} \cdot \text{H}_2\text{O}$ and $\text{Ag}_7\text{I}_2\text{F}_5 \cdot 2.5\text{H}_2\text{O}$. Such short O . . . F distances (about 2.50 Å) have also been observed in some other compounds, e.g., $\text{Fe}(\text{H}_2\text{O})_6\text{F}_2$ (29), $\text{HgF}_2 \cdot 2\text{H}_2\text{O}$ (30), $\text{Te}(\text{OH})_6 \cdot \text{NaF}$ (31), and $\text{Hg}(\text{OH})\text{F}$ (32), and even shorter distances—e.g., 2.38 Å in $\text{K}[\text{PHO}_2(\text{OH})] \cdot \text{HF}$ (33)—have been found. These structures, containing short (<2.6 Å) O . . . F hydrogen bonds, were studied with X-ray diffraction and hence the H atom positions are not determined accurately, if at all.

The O–H distances, determined from neutron data, in $\text{Ag}_2\text{IF} \cdot \text{H}_2\text{O}$ are comparably long: 1.03 and 1.16 Å, respectively, the longest one corresponding to the shortest O–H . . . F distance. It is known that the H atom has a more symmetrical position between the O atoms in shorter O–H . . . O bonds of about 2.50 Å than in longer ones. This in turn results in an elongation of the O–H distance; values up to 1.1 Å are not unusual (26). This relation might also be true for O–H . . . F bonds and the difference in the O–H distances in $\text{Ag}_2\text{IF} \cdot \text{H}_2\text{O}$ can thus be looked upon as a manifestation of a more general effect. Among the compounds containing O–F hydrogen bonds, which have been studied with neutron diffraction, there seems to be no example of O–F distances shorter than 2.56 Å (in $\text{ZnF}_2 \cdot 4\text{H}_2\text{O}$ (34)). In these

longer bonds the O–H distances fall in the range 0.9–1.0 Å.

The Coordination of Ag to I

The I atom is located in a rectangular box of eight Ag atoms. Four of these Ag atoms are much closer in distance (Table III) and the "coordination polyhedron" can be described as a square pyramid containing two Ag_2 pairs in the corners of the base plane and the I atom at the top. Such pyramids share Ag–Ag edges, forming a chain along **b**, where the top iodine atom alternates from one side of the Ag plane to the other (Fig. 6). The Ag–I distances are in the same order of magnitude as those found in $\beta\text{-AgI}$ (2.814 Å (35)) and the shortest Ag–I in $\text{Ag}_7\text{I}_2\text{F}_5 \cdot 2.5\text{H}_2\text{O}$ (13).

Previous studies have shown that stoichiometrically similar compounds of the $\text{Ag}_n\text{X}_x\text{A}_y$ family may have different Ag-to-X coordination depending on A. This is true for $\text{Ag}_3\text{I}(\text{NO}_3)_2$ and $\text{Ag}_3\text{I}(\text{ClO}_4)_2 \cdot 2\text{H}_2\text{O}$, with distorted trigonal prisms Ag_6I (5) and Ag_7I_2 units containing a bridging I–Ag–I segment between two terminal Ag_3 groups (6), respectively. By comparison with Ag_2INO_3 (4) with distorted trigonal Ag_6 prisms around I, the structure of $\text{Ag}_2\text{IF} \cdot \text{H}_2\text{O}$ also clearly demonstrates the importance of the nature of the counterion A for the coordination of Ag to I. Further, it should be noted that the variation in overall stoichiometry from $\text{Ag}_2\text{IF} \cdot \text{H}_2\text{O}$ to $\text{Ag}_7\text{I}_2\text{F}_5 \cdot 2.5\text{H}_2\text{O}$ also brings about changes in the short-range arrangement of Ag around I. The I atoms of the latter compound are rather unsymmetrically sur-

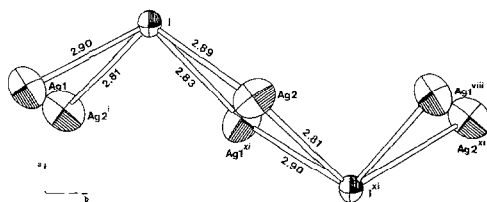


FIG. 6. A part of the Ag_2I^+ chain.

rounded by seven and eight Ag atoms (13). These observations lead to the conclusion that there are no strong directional demands on the Ag–I bonds in $\text{Ag}_n\text{I}_x\text{A}_y$ compounds, although the Ag–I distances are generally of an order of magnitude that might be classified as covalent. It seems rather that ion packing effectively governs the structure building.

The Ag–Ag Pairs

As mentioned above, the Ag^+ ions of $\text{Ag}_2\text{IF} \cdot \text{H}_2\text{O}$ are grouped together to Ag(1)–Ag(2) pairs with an Ag–Ag distance of 2.81 Å, which is remarkably short as compared to 2.89 Å in silver metal (36). This might be taken as an indication of an intermetallic interaction within the Ag_2 pairs. Another remarkably short Ag–Ag distance, occurring across a shared I–I edge of two tetrahedra around the Ag atoms, has also been found in $\text{SrAg}_2\text{I}_4 \cdot 8\text{H}_2\text{O}$ (37). Short Ag–Ag distances have previously been found in compounds containing silver in a formal oxidation state lower than +1, e.g., Ag_2F (38)

TABLE V

COMPOUNDS WITH Ag(I)–Ag(I) DISTANCES $d_{\text{Ag–Ag}} \leq 2.89$ Å, THE Ag–Ag SEPARATION IN SILVER METAL

Compound	$d_{\text{Ag–Ag}}$ (Å)	Ref.
Ag_3PO_4	2.77(1) ^a	(42)
$(\text{C}_{10}\text{H}_{21}\text{AgO}_3)_2 \cdot 2\text{H}_2\text{O}$	2.778(5), 2.834(5)	(57)
$\text{SrAg}_2\text{I}_4 \cdot 8\text{H}_2\text{O}$	2.78(1) ^b	(37)
$\text{Ag}_2\text{IF} \cdot \text{H}_2\text{O}$	2.812(2)	This work
SrAg_6O_4	2.81, 2.84	(43)
AgHg_2PO_4	2.824(4)	(44)
$\text{AgCNO}(\text{trig.})$	2.82	(45)
LiAg_3O_2	2.84	(46)
BaAg_6O_4	2.84, 2.89	(47)
$\text{Ag}_2(\text{C}_3\text{H}_2\text{O}_4)$	2.851(1)	(58)
$(\text{AgC}_2\text{F}_3\text{O}_2)_2 \cdot \text{C}_6\text{H}_6$	2.859(3), 2.893(3)	(48)
$\beta\text{-Ag}_4\text{Te}(\text{NO}_3)_2$	2.86	(49)
Ag_2CO_3	2.873(2)	(50)
$\text{Ag}_4\text{SO}_2\text{N}_2$	2.87, 2.89	(51)
$\text{AgNO}_3 \cdot \text{NH}_2\text{CH}_2\text{COOH}$	2.877(6)	(52)
$\alpha\text{-Ag}_4\text{Te}(\text{NO}_3)_2$	2.89(1)	(53)
Ag_6SiS_6	2.890	(54)
$\text{Ag}_2(\text{SO}_3\text{CH}_2\text{CH}_2\text{SO}_3)$	2.891(1)	(55)

^a Distance between Ag sites with an occupancy factor of $\frac{1}{2}$.

^b The $\text{Ag}^+ \text{--} \text{Ag}^+$ distance is across an $\text{I}^- \text{--} \text{I}^-$ edge as in $\text{Ag}_2\text{IF} \cdot \text{H}_2\text{O}$.

TABLE VI

XPS DATA FOR $\text{Ag}_2\text{IF} \cdot \text{H}_2\text{O}$ AND RELATED SUBSTANCES. ALL VALUES ARE REFERRED TO $\text{C1s} = 285.0$ eV

Substance	Electron-binding energy (eV)		
	$\text{Ag}3d_{5/2}$	$\text{I}3d_{5/2}$	$\text{F}1s$
$\text{Ag}_2\text{IF} \cdot \text{H}_2\text{O}$	368.0	619.1	681.8
AgI	368.4	619.2	
AgF	367.5		682.0
Ag	368.2		

(2.81 Å), $\text{Ag}_{1-x}\text{V}_2\text{O}_5$ (39) (2.77 Å), and $\text{Ag}_6\text{Ge}_{10}\text{P}_{12}$ (40) (2.85 Å). In recent years, however, a number of compounds with Ag(I)–Ag(I) distances ≤ 2.89 Å have been reported, and the Ag substructure in oxocompounds with short Ag(I)–Ag(I) distances has recently been treated in a review by Jansen (41). A number of compounds known to have Ag(I)–Ag(I) distances ≤ 2.89 Å are collected in Table V. It is evident from the table that extremely short Ag(I)–Ag(I) distances occur rather frequently and that this phenomenon is not restricted to the oxocompounds treated by Jansen (41). The 2.81 Å distance in $\text{Ag}_2\text{IF} \cdot \text{H}_2\text{O}$ is one of the shortest Ag(I) separations observed, and the whole Ag substructure can effectively be described as built up of Ag_2^{2+} pairs.

An attempt was made to trace the effects of a possible intermetallic orbital interaction on the electron binding energies by recording X-ray photoelectron spectra of $\text{Ag}_2\text{IF} \cdot \text{H}_2\text{O}$ and the parent compounds AgI and AgF. The results, pertaining to the levels $\text{Ag}3d_{5/2}$, $\text{I}3d_{5/2}$, and $\text{F}1s$, are given in Table VI, together with the value for metallic silver for comparison. No perturbation of the $\text{Ag}3d$ bandshape could be detected, and the shifts in the $\text{Ag}3d_{5/2}$ binding energies are strikingly regular in the sequence $\text{AgF} \text{--} \text{Ag}_2\text{IF} \cdot \text{H}_2\text{O} \text{--} \text{AgI}$, whereas the $\text{I}3d_{5/2}$ and $\text{F}1s$ binding energies are little influenced by the chemical changes. The data thus furnish no evidence for interme-

tallic interactions. Attempts at a characterization of the $\text{Ag}4d$ valence band were also made, but the instrument resolution did not permit any definite conclusion based on differences in bandshape. High-resolution methods, such as uv photoelectron spectroscopy, might possibly be more informative in detecting the extent of intermetallic orbital interaction in compounds with extremely small Ag(I) separation.

Acknowledgments

Professors Ido Leden and Sten Andersson and Dr. Åke Oskarsson have supported this work with discussions and helpful advice which is greatly appreciated. Drs. Roland Tellgren and John O. Thomas and Ing. Stig Lundholm made the collection of neutron data possible. We also thank Dr. Börje Folkesson for recording the XPS data. This work is part of a project supported by the Swedish Natural Science Research Council.

References

1. A. SCHIRALDI, *Electrochim. Acta* **23**, 1039 (1978).
2. K. PERSSON, *Acta Crystallogr. Sect. B* **35**, 1432 (1979).
3. K. PERSSON AND B. HOLMBERG, *Acta Crystallogr. Sect. B* **33**, 3768 (1977).
4. K. PERSSON, *Acta Crystallogr. Sect. B* **35**, 302 (1979).
5. R. BIRNSTOCK AND D. BRITTON, *Z. Kristallogr.* **132**, 87 (1970).
6. K. PERSSON AND B. HOLMBERG, to be published.
7. L. Y. Y. CHAN AND S. GELLER, *J. Solid State Chem.* **21**, 331 (1977).
8. K. PERSSON AND B. HOLMBERG, *Acta Crystallogr. Sect. B* **38** (1982), in press.
9. B. HOLMBERG, *Acta Chem. Scand. Ser. A* **30**, 680 (1976).
10. K. H. LIESER, *Z. Anorg. Chem.* **305**, 133 (1960).
11. E. HAYEK, *Monatsh. Chem.* **68**, 29 (1936).
12. B. HOLMBERG AND K. PERSSON, *Acta Crystallogr. Sect. A* **31**, S65 (1975).
13. K. PERSSON AND B. HOLMBERG, *Acta Crystallogr. Sect. B* **38** (1982), in press.
14. R. KARLSSON, *Talanta* **19**, 1639 (1972).
15. I. ELDDING, *Acta Chem. Scand. Ser. A* **30**, 649 (1976).
16. S. DANIELSSON, I. GRENTHE, AND Å. OSKARSSON, *J. Appl. crystallogr.* **9**, 14 (1976).
17. J. KARLE AND I. L. KARLE, *Acta Crystallogr.* **16**, 969 (1963).
18. J. KARLE AND I. L. KARLE, *Acta Crystallogr. Sect. B* **25**, 925 (1966).
19. D. T. CROMER AND J. T. WABER, "International Tables for X-ray Crystallography," Vol. IV, Kynoch Press, Birmingham (1974).
20. W. H. ZACHARIASEN, *Acta Crystallogr.* **23**, 556 (1967).
21. S. C. ABRAHAMS AND T. KEVE, *Acta Crystallogr. Sect. A* **27**, 157 (1971).
22. G. E. BACON, *Acta Crystallogr. Sect. A* **28**, 357 (1972).
23. R. M. MOON AND C. G. SHULL, *Acta Crystallogr.* **17**, 805 (1963).
24. H. SCHULZ AND K. H. THIEMANN, *Acta Crystallogr. Sect. A* **35**, 309 (1979).
25. C. GREAVES AND B. E. F. FENDER, *Acta Crystallogr. Sect. B* **28**, 3609 (1972).
26. C. PIMENTEL AND A. L. MCCLELLAND, *Annu. Rev. Phys. Chem.* **22**, 355 (1971).
27. V. J. SIMONOV AND B. V. BUKVETSKII, *Acta Crystallogr. Sect. B* **34**, 355 (1978).
28. H. KISTENMACHER, H. POPKIE, AND E. CLEMENTI, *J. Chem. Phys.* **58**, 5627 (1973).
29. B. R. PENFOLD AND M. R. TAYLOR, *Acta Crystallogr.* **13**, 953 (1960).
30. B. V. BUKVETSKII, S. A. POLISHCHUK, AND V. I. SIMONOV, *Koord. Khim.* **2**, 1208 (1976).
31. R. ALLMANN, *Acta Crystallogr. Sect. B* **32**, 1025 (1976).
32. C. STÅLHANDSKE, *Acta Crystallogr. Sect. B* **35**, 949 (1979).
33. H. ALTENBURG AND D. MOOTZ, *Acta Crystallogr. Sect. B* **27**, 1982 (1973).
34. B. V. BUKVETSKII, YU. Z. NOZIK, L. E. FYKIN, S. A. POLISHCHUK, AND N. M. NAPTASH, *Koord. Khim.* **3**, 1594 (1977).
35. G. BURLEY, *J. Chem. Phys.* **38**, 2807 (1963).
36. M. E. STRAUMANIS AND S. M. RIAD, *Trans. AIME* **233**, 964 (1965).
37. S. GELLER AND T. O. DUDLEY, *J. Solid State Chem.* **26**, 321 (1978).
38. G. Y. ARGAY AND I. NÁRAY-SZABÓ, *Acta Chim. Acad. Sci. Hung.* **49**, 329 (1966).
39. S. ANDERSSON, *Acta Chem. Scand.* **19**, 1371 (1965).
40. H. G. VON SCHNERING AND K.-G. HÄUSLER, *Rev. Chim. Min.* **13**, 71 (1976).
41. M. JANSEN, *J. Less-Common Met.* **76**, 285 (1980).
42. H. N. NG, C. CALVO, AND R. FAGGIANI, *Acta Crystallogr. Sect. B* **34**, 898 (1978).
43. H.-L. KELLER AND H. K. MÜLLER-BUSCHBAUM, *Z. Anorg. Allg. Chem.* **393**, 266 (1972).
44. R. MASSE, J.-C. GUITEL, AND A. DURIF, *J. Solid State Chem.* **23**, 369 (1978).
45. D. BRITTON AND J. D. DUNITZ, *Acta Crystallogr.* **19**, 662 (1965).

46. M. JANSEN, *Z. Naturforsch. B* **30**, 854 (1975).
47. H.-L. KELLER AND H. K. MÜLLER-BUSCHBAUM, *Z. Naturforsch. B* **28**, 263 (1973).
48. G. W. HUNT, T. C. LEE, AND E. L. AMMA, *Inorg. Nucl. Chem. Lett.* **10**, 909 (1974).
49. E. SCHULTZE-RHONHOF AND G. BERGERHOFF, *Acta Crystallogr. Sect. B* **25**, 2645 (1969).
50. R. MASSE, J.-C. GUITEL, AND A. DURIF, *Acta Crystallogr. Sect. B* **35**, 1428 (1979).
51. C. KRATKY AND A. POPITSCH, *Acta Crystallogr. Sect. B* **36**, 1044 (1980).
52. J. K. H. RAO AND H. A. VISWAMITRA, *Acta Crystallogr. Sect. B* **28**, 1484 (1972).
53. E. SCHULTZE-RHONHOF, *Acta Crystallogr. Sect. B* **31**, 2837 (1975).
54. B. KREBS AND J. MANDT, *Z. Naturforsch. B* **32**, 373 (1977).
55. F. CHARBONNIER, R. FAURE, AND H. LOISELEUR, *Acta Crystallogr. Sect. B* **37**, 822 (1981).
56. C. K. JOHNSON, ORTEP II. Report ORNL-3794, Oak Ridge National Laboratory, Oak Ridge, Tenn. (1971).
57. P. COGGON AND A. T. MCPHAIL, *J. Chem. Soc. Chem. Commun.* **91** (1972).
58. F. CHARBONNIER, R. FAURE, AND H. LOISELEUR, *Rev. Chim. Miner.* **18**, 245 (1981).